PHYSICAL REVIEW A **86**, 051402(R) (2012)

Efficient ground-state cooling of an ion in a large room-temperature linear Paul trap with a sub-Hertz heating rate

G. Poulsen, Y. Miroshnychenko, and M. Drewsen

QUANTOP–The Danish National Research Foundation Center for Quantum Optics, Department for Physics and Astronomy, Aarhus University, Aarhus, Denmark

(Received 9 May 2012; published 26 November 2012)

We demonstrate efficient resolved sideband laser cooling (99 ± 1% ground-state population) of a single $^{40}Ca^{+}$ ion in a large linear Paul trap (electrode spacing of 7 mm) operated at an rf drive frequency of just 3.7 MHz. For ion oscillation frequencies in the range 280–585 kHz, heating rates below or about one motional quantum per second have been measured at room temperature. The results, obtained under these unconventional sideband cooling conditions, pave the way for a range of new types of cold ion experiments, including spectroscopy of molecular ions as well as ultracold chemistry.

DOI: 10.1103/PhysRevA.86.051402 PACS number(s): 37.10.Rs, 37.10.Ty, 37.10.Vz

Resolved sideband laser cooling of trapped atomic ions was originally proposed with the aim of improving optical spectroscopy [1]. Since the first experimental demonstrations of this technique [2], single-ion cooling to the ground state of the trapping potential has been performed both in one [2] and three dimensions [3], with a record high one-dimensional ground-state population of 99.9% [4]. The possibility of sideband cooling several simultaneously trapped ions [5,6] furthermore has recently led to a number of outstanding results within quantum information science (see, e.g., Refs. [7,8] and references therein) and ultraprecise ion spectroscopy [9–11]. While narrow ionic electronic transitions may eventually be applied to establish new, improved optical atomic clocks, the extreme spectral resolution obtainable with sideband cooled ions enables also fundamental physics investigations, including the search for a potential time variation of natural constants (e.g., the fine-structure constant [12,13] and the proton-to-electron mass ratio [14,15]), and a potential electric dipole moment of the electron [16].

For all of the above-mentioned applications, uncontrolled interactions between the trapped ions and the environment are key issues for the final quality of the measurements. For instance, fluctuating electrical patch potentials on the trapping electrodes will lead to heating of the ion motion [17], and limit the potential interrogation time. A simple model of this effect predicts heating rates which scale roughly inversely with the distance from the ions to the electrodes to the power of four [17], a dependence consistent with experimental findings for traps at room temperature [18]. For scalable quantum information processing with trapped ions which requires small traps, currently the only viable solutions to this problem seem to be applying microtraps cooled to cryogenic temperatures [19], or using trap electrodes which can be cleaned *in situ* [20]. For a large range of other applications such as the spectroscopy of molecular ions [21,22] and ultracold ion chemistry [23–27], typically with only one target and one coolant ion trapped simultaneously, an alternative, simpler strategy could be just to employ larger traps at room temperature. In this Rapid Communication, we report on one-dimensional ground-state sideband laser cooling of a single $^{40}Ca^{+}$ ion in a room-temperature linear radio-frequency trap with a radial diagonal electrode spacing of 7.0 mm and an rf drive frequency of just 3.7 MHz. In other words, the trap has an ion-electrode spacing about three times larger and an rf frequency nearly a factor of 2 lower than reported in previous ground-state cooling experiments. In this trap, we have demonstrated very efficient cooling (99 ± 1% final ground-state population) and measured motional heating rates over months around one motional quantum per second for oscillation frequencies in the range of 280–585 kHz. For the prospect of high-resolution spectroscopy of molecular ions by quantum logic spectroscopy (QLS) [9], these results are very promising. First, the extremely low heating rates make it possible to investigate very narrow and weak molecular transitions, since long interaction times can be allowed for without motional decoherence. Second, the very efficient ground-state cooling suggests that clean QLS signals should be obtainable. Third, ground-state cooling of ions at oscillation frequencies of only a few hundred of kHz makes it possible not only to apply QLS to electronic transitions in the visible range, but also to vibrational transition in the near- and mid-infrared region since relatively large Lamb Dicke parameters are achievable. For spectroscopy in the UV range, higher oscillation frequencies though are needed to avoid unwanted off-resonant higher-order sideband excitations. The required increased oscillation frequency could in principle be achieved by applying a higher rf frequency to the existing trap, but in order to reduce the necessary rf voltage, it might be favorable to reduce the dimension of the trap, e.g., by a factor of 2 (the needed rf voltage scales quadratically with trap dimensions).

The large dimensions of our trap furthermore ensure a relative deep trap potential (∼5 eV) despite the low oscillation frequencies, making it possible to trap and cool molecular ions formed through reactions with large excess kinetic energy release. In addition, operating the trap at low rf frequency requires only modest rf voltages.

The low zero-point energy associated with the ground-state cooled ion at these low oscillation frequencies (∼7 μK for an oscillation frequency of 280 kHz) also make this trap an interesting tool for investigations of ultracold ion chemistry [23–27]. In this connection, it should be mentioned that we have been able to minimize the amplitudes of the rf sidebands due to uncompensated rf fields to a level corresponding to a residual micromotion energy equivalent to a temperature below 1 μK in all three dimensions. Finally, the large and very

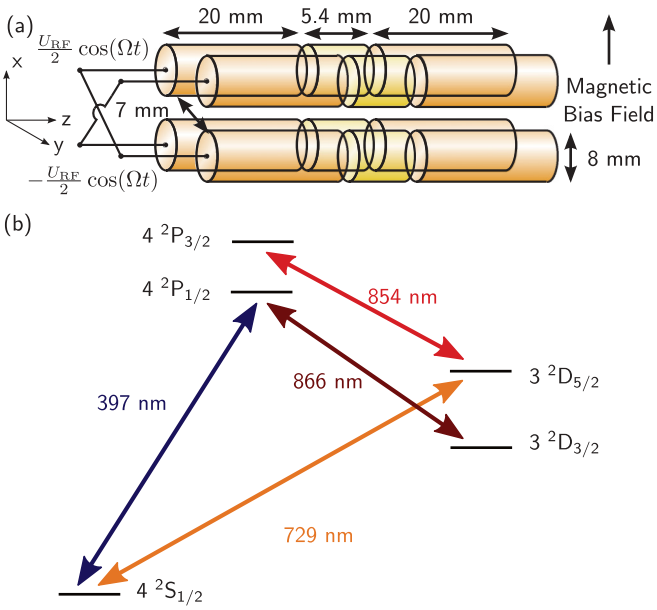

FIG. 1. (Color online) (a) Sketch of the macroscopic linear Paul trap including dimensions of and electrical potentials on the electrodes. The electrodes have, in addition to the rf potential, a dc potential for axial confinement. The orientation of the applied magnetic bias field is also indicated. (b) Reduced level scheme for $^{40}Ca^+$ with indication of the transitions addressed under Doppler and sideband cooling. For details, see the main text.

open trap geometry is ideal for combining the trap setup with magneto-optical traps (MOTs) [26,27], cold molecule sources such as Stark [28] and Zeeman [29] decelerators, as well as velocity filters [30,31].

In Fig. 1, a sketch of the linear rf trap (for details on the trap design, see Ref. [32]) as well as a reduced level scheme of the $^{40}Ca^+$ ion with indications of the laser-driven transitions are presented. The linear trap consists of four segmented stainless-steel cylindrical electrodes plated with 5-μm gold to which rf potentials are provided in a symmetrical fashion to create an effective radial trapping potential. Axial confinement is achieved through application of an additional dc potential to all eight end-sections of the electrodes. Furthermore, smaller dc and rf offset potentials can be applied independently to all 12 sections to minimize rf micromotion at the effective trap potential center. The rf amplitude can reach 1.5 kV and the dc potentials can be raised to 100 V. For typical single-ion experiments, the trap is operated with $U_{rf} = 1.2$ kV and an endcap potential of $U_z = 20$–80 V, which results in axial and radial secular oscillation frequencies of $\nu_z = 280$–585 kHz and $\nu_{x,y} = 1$ MHz, respectively. In all experiments, a bias magnetic field of 6 G is applied along the x direction. Prior to all sideband cooling experiments, the micromotion is minimized to at least a modulation index below 10^{-1} in all directions (along the quadrupole symmetry axis, the z axis, it is even compensated down to 10^{-3}) by measuring the Rabi oscillation frequencies on the micromotion sidebands.

A typical experimental cooling cycle starts with a 5 ms period of Doppler cooling by addressing the $S_{1/2} \leftrightarrow P_{1/2}$ transition of the ion with a 397-nm laser beam propagating along the $\frac{1}{\sqrt{2}}(\hat{x} + \hat{y})$ direction, and repumping population out

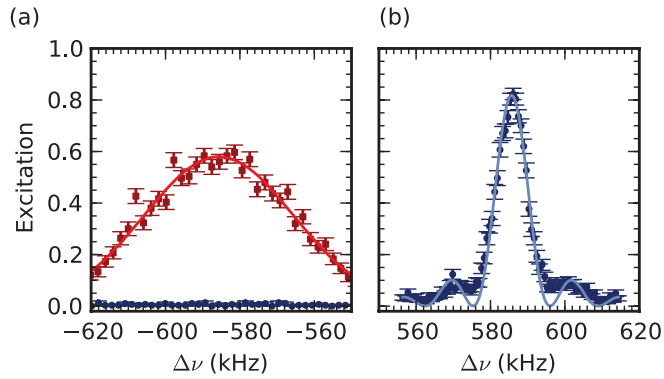

FIG. 2. (Color online) (a) First-order red sideband excitation spectra before (red solid squares) and after (blue solid circles) sideband cooling at an axial oscillation frequency of 585 kHz. (b) Corresponding first-order blue sideband excitation spectrum after sideband cooling (blue solid circles). $\Delta\nu$ is the frequency detuning with respect to the carrier, and the vertical axis indicates the population transfer to the $D_{5/2}$ level due to the sideband excitation pulse. A quantitative analysis of the measured strengths indicates a 0.99 ± 0.01 population of the motional ground state. The presented curves are fits to a Gaussian and Rabi line shape, respectively.

of the $D_{3/2}$ state by a 866-nm laser beam propagating along the $\hat{z}$ direction. This is followed by an 8 ms sideband cooling period comprising successive pairs of pulses addressing the red sidebands of the $S_{1/2}(m_J = -1/2) \leftrightarrow D_{5/2}(m_J = -5/2)$ transition and the sideband unresolved $D_{5/2} \leftrightarrow P_{3/2}$ transition. The cooling sequence starts with 200 cycles on the second red sideband followed by 200 cycles on the first red sideband. Finally, the optical intensity is lowered for another 25 cooling cycles on the first red sideband to minimize the effect of off-resonant scattering on the carrier transition. During the whole sideband cooling sequence, every 25 cooling cycles are followed by pulses driving the $S_{1/2}(m_J = +1/2) \leftrightarrow D_{5/2}(m_J = -1/2)$ and the $D_{5/2} \leftrightarrow P_{3/2}$ transitions to avoid trapping in the $S_{1/2}(m_J = +1/2)$ state. (The $D_{5/2} \leftrightarrow P_{3/2}$ and $D_{3/2} \leftrightarrow P_{1/2}$ transitions are always driven together to avoid optical pumping into the $D_{3/2}$ level.)

The ground state population is determined by comparing the spectra of the first red and blue sidebands of the $S_{1/2} \leftrightarrow D_{5/2}$ transition using the standard electron shelving technique [4]. In Fig. 2, examples of such spectra are presented for an experiment performed with $U_{rf} = 1.2$ kV and $U_{dc} = 80$ V, corresponding to $\nu_z = 585$ kHz. In Fig. 2(a), the red sideband spectrum is presented both before and after sideband cooling. After cooling, this sideband clearly vanishes in contrast to the blue sideband presented in Fig. 2(b). A suppressed sideband could in principle also originate from population in excited motional states with vanishing coupling or pulses corresponding to 2π rotations. However, with cooling on both the second and first sideband (the latter at different powers) and the chosen pulse lengths, such potential trapping states are avoided. A quantitative comparison between the two cooled sideband spectra leads to the conclusion that the ion has an average ground-state population of 0.99 ± 0.01, corresponding to a temperature of 6^{+1}_{-6} μK.

To gain information on the reheating of the ion in the trap, the red and blue sideband spectra have been compared

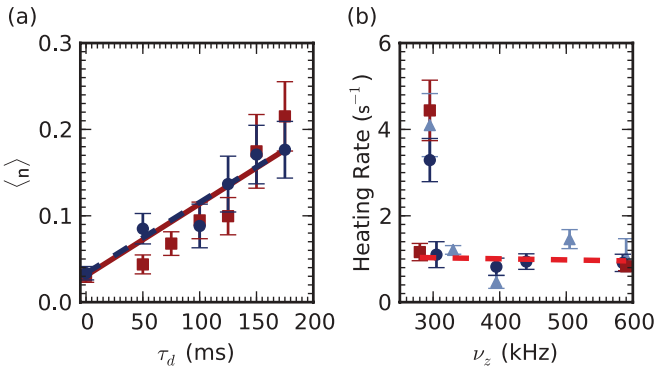

FIG. 3. (Color online) (a) The mean occupation number of motional excitation $\langle n\rangle$ vs time τ_d after ended sideband cooling with an axial oscillation frequency $\nu_z = 585$ kHz. The red solid squares (blue solid circles) represent data points without (with) a mechanical shutter for blocking 397-nm light (see text for details). The solid red and dashed blue lines are best linear fits to the two data sets, resulting in heating rates of $d\langle n\rangle/dt = 0.83 \pm 0.10\ \mathrm{s}^{-1}$ and $d\langle n\rangle/dt = 0.84 \pm 0.05\ \mathrm{s}^{-1}$. (b) Measured heating rates vs axial oscillation frequency. The navy blue circles represent data points obtained the same day, while the light blue triangular data points are obtained during a period of 2 months. The red squares represent alternative rf voltages to rule out parametric resonances. A constant fit to all data points except the ones at the "resonance" at 295 kHz gives a heating rate of $1.1 \pm 0.35\ \mathrm{s}^{-1}$.

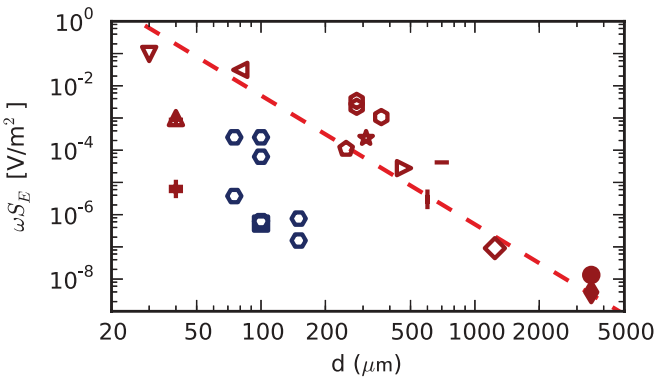

FIG. 4. (Color online) Heating rate measurements in terms of the spectral noise density multiplied by the oscillation frequency (ωS_E) versus the shortest distance (d) between the ion and the trap electrodes. Previous results from cooled (○ and □) and room temperature traps (all others) are presented together with some of our results (● $\nu_z = 585$ kHz and ♦ $\nu_z = 280$ kHz). Obviously, the value of ωS_E for our experiments with $\nu_z = 280$ kHz are more than one order of magnitude lower than previously measured, while at the same time our results generally follow the $1/d^4$ scaling (dashed line) expected for fluctuating patch potentials. △ ^{24}Mg$^+$, Au [34]; ▽ ^{111}Cd$^+$, GaAs [35]; ◁ ^{137}Ba$^+$, Be-Cu [36]; ▷ ^{198}Hg$^+$, Mo [2]; ▮ ^{40}Ca$^+$, Mo [4]; ✿ ^{40}Ca$^+$, Au [37]; ▬ ^{171}Yb$^+$, Mo [38]; ★ ^{174}Yb$^+$, Au [39]; ⬡ ^{9}Be$^+$, Au [17]; ○ ^{88}Sr$^+$, Ag 6K [19]; □ ^{88}Sr$^+$, Al 6K [40]; ◇ ^{43}Ca$^+$, St. Steel [41]; ✚ ^{9}Be$^+$, Au [20]; ● ^{40}Ca$^+$, Au ♦ ^{40}Ca$^+$, Au.

at different delays after cooling. from which the mean occupation number $\langle n\rangle$ has been evaluated. Results from such measurements are presented in Fig. 3(a) for trapping conditions identical to those above. As evident from the data, the heating rates are found to be below one quantum per second. The slight offset from $\langle n\rangle = 0$ at short delays arises from nonoptimized initial sideband cooling.

To test whether this low heating rate is particular to the chosen axial oscillation frequency, similar experiments were conducted for other trapping parameters. In Fig. 3(b), the results in terms of measured heating rates as a function of ν_z in the interval 280–585 kHz are presented. Obviously, the heating rate seems to be essentially independent of the oscillation frequency and only amounts to one quantum per second, except for the case of $\nu_z = 295$ kHz. The low heating rates have been found to be very persistent, and several of the points in Fig. 3(b) indeed have been measured over months. This includes the resonance at 295 kHz, which has also been proven to be independent of the rf voltage applied, indicating that it is not caused by some particular nonlinear resonances due to an imperfect trap [33].

In Fig. 4, our heating rate measurements are compared with ones from other trap experiments on the basis of deduced spectral noise densities. In terms of the product of the spectral noise density and the ion oscillation frequency, our results surpass previous ones obtained in room temperature as well as cryogenic traps by more than an order of magnitude.

Our measured ultralow heating rates seem to follow the generally accepted $1/d^4$ scaling, where d is the nearest distance from the ion to the electrodes. The dominating contribution is, however, probably from technical noise and not fluctuating patch potentials, since the measured heating rates are found to be independent of the oscillation frequency [17].

The primary source of motional heating is at present not clear, but a series of experiments have been conducted to rule out a few. For instance, in Fig. 3(a), the two data sets represent two experimental runs with the only difference being the 397-nm light used for Doppler cooling being turned off completely by a mechanical shutter after 15 ms instead of just shut off from a level of 45 mW/cm^2 by an acousto-optical modulator (>70 dB extinction) for the one set of data. Apparently, the non-completely shutting of 397 nm light have no significant influence on the heating. Spectrum analysis of the rf and dc source have also been carried out without any indication of a noise spectral density increasing linearly with the oscillation frequency as could be expected from our measured constant heating rates and the theory presented in Ref. [17]. The resonance around 295 kHz though has been identified to be caused by a switch-mode power supply applied in a neighbor experiment.

Though spontaneous emission in connection with sideband cooling at the low trap frequencies applied in our experiments will lead to heating of the unaddressed motional degrees of freedom, the low heating rates imply that it should be feasible to cool all degrees of freedom to the motional ground state (of a single ion or more) by sequential sideband cooling. Hence, experiments involving a single sympathetically sideband cooled ion in our type of trap should enable both high-resolution quantum logic spectroscopy of, e.g., highly charged [12] and molecular ions [21], and ion chemistry in the ultracold regime [23]. With respect to the latter prospect, the low heating rates should additionally make it possible to adiabatically lower the trap potential to reach temperatures lower than might be reached by direct sideband cooling. The large dimensions of our trap furthermore makes it very versatile as it allows easy introduction

of multiple laser beams as well as particle beams without facing the problem of exposing surfaces close to the ions.

In conclusion, we have demonstrated that it is possible to carry out effective ground-state sideband cooling in macroscopic linear rf traps with low rf drive frequencies operated at room temperature. The low heating rates indicate that such a trap could be the proper choice for many experiments concerning quantum logic spectroscopy and ultracold chemistry.

[1] D. J. Wineland and H. Dehmelt, Bull. Am. Phys. Soc. **20**, 637 (1975).
[2] F. Diedrich, J. C. Bergquist, W. M. Itano, and D. J. Wineland, Phys. Rev. Lett. **62**, 403 (1989).
[3] C. Monroe, D. M. Meekhof, B. E. King, S. R. Jefferts, W. M. Itano, D. J. Wineland, and P. Gould, Phys. Rev. Lett. **75**, 4011 (1995).
[4] C. Roos, T. Zeiger, H. Rohde, H. C. Nägerl, J. Eschner, D. Leibfried, F. Schmidt-Kaler, and R. Blatt, Phys. Rev. Lett. **83**, 4713 (1999).
[5] B. E. King, C. S. Wood, C. J. Myatt, Q. A. Turchette, D. Leibfried, W. M. Itano, C. Monroe, and D. J. Wineland, Phys. Rev. Lett. **81**, 1525 (1998).
[6] H. Rohde, S. T. Gulde, C. F. Roos, P. A. Barton, D. Leibfried, J. Eschner, F. Schmidt-Kaler, and R. Blatt, J. Opt. B **3**, S34 (2001).
[7] P. Schindler, J. T. Barreiro, T. Monz, V. Nebendahl, D. Nigg, M. Chwalla, M. Hennrich, and R. Blatt, Science **332**, 1059 (2011)
[8] C. Ospelkaus, U. Warring, Y. Colombe, K. R. Brown, J. M. Amini, D. Leibfried, and D. J. Wineland, Nature (London) **476**, 181 (2011).
[9] P. O. Schmidt, T. Rosenband, C. Langer, W. M. Itano, J. C. Bergquist, and D. J. Wineland, Science **309**, 749 (2005).
[10] C. W. Chou, D. B. Hume, J. C. J. Koelemeij, D. J. Wineland, and T. Rosenband, Phys. Rev. Lett. **104**, 070802 (2010).
[11] C. W. Chou, D. B. Hume, T. Rosenband, and D. J. Wineland, Science **329**, 1630 (2010).
[12] S. Schiller, Phys. Rev. Lett. **98**, 180801 (2007).
[13] T. Rosenband, D. B. Hume, P. O. Schmidt, C. W. Chou, A. Brusch, L. Lorini, W. H. Oskay, R. E. Drullinger, T. M. Fortier, J. E. Stalnaker, S. A. Diddams, W. C. Swann, N. R. Newbury, W. M. Itano, D. J. Wineland, and J. C. Bergquist, Science **319**, 1808 (2008).
[14] S. Schiller and V. Korobov, Phys. Rev. A **71**, 032505 (2005).
[15] V. V. Flambaum and M. G. Kozlov, Phys. Rev. Lett. **99**, 150801 (2007).
[16] L. C. Sinclair, K. C. Cossel, T. Coffey, J. Ye, and E. A. Cornell, Phys. Rev. Lett. **107**, 093002 (2011).
[17] Q. A. Turchette, D. Kielpinski, B. E. King, D. Leibfried, D. M. Meekhof, C. J. Myatt, M. A. Rowe, C. A. Sackett, C. S. Wood, W. M. Itano, C. Monroe, and D. J. Wineland, Phys. Rev. A **61**, 063418 (2000).
[18] N. Daniilidis, S. Narayanan, S. A. Möller, R. Clark, T. E. Lee, P. J. Leek, A. Wallraff, S. Schulz, F. Schmidt-Kaler, and H. Häffner, New J. Phys. **13**, 013032 (2011).
[19] J. Labaziewicz, Y. Ge, P. Antohi, D. Leibrandt, K. R. Brown, and I. L. Chuang, Phys. Rev. Lett. **100**, 013001 (2008).
[20] D. A. Hite, Y. Colombe, A. C. Wilson, K. R. Brown, U. Warring, R. Jördens, J. D. Jost, K. S. McKay, D. P. Pappas, D. Leibfried, and D. J. Wineland, Phys. Rev. Lett. **109**, 103001 (2012).
[21] P. O. Schmidt, T. Rosenband, J. C. J. Koelemeij, D. B. Hume, W. M. Itano, J. C. Bergquist, and D. J. Wineland, in *Non-Neutral Plasma Physics VI: Workshop on Non-Neutral Plasmas 2006*, edited by M. Drewsen, U. Uggerhoj, and H. Knudsen, AIP Conf. Proc. No. **862** (AIP, Melville, NY, 2006), p. 305.
[22] I. S. Vogelius, L. B. Madsen, and M. Drewsen, J. Phys. B **39**, S1259 (2006).
[23] S. Willitsch, M. T. Bell, A. D. Gingell, and T. P. Softley, Phys. Chem. Chem. Phys. **10**, 7200 (2008).
[24] R. Côté, V. Kharchenko, and M. D. Lukin, Phys. Rev. Lett. **89**, 093001 (2002).
[25] Z. Idziaszek, T. Calarco, P. S. Julienne, and A. Simoni, Phys. Rev. A **79**, 010702 (2009).
[26] C. Zipkes, S. Palzer, C. Sias, and M. Kohl, Nature (London) **464**, 388 (2010).
[27] S. Schmid, A. Härter, and J. H. Denschlag, Phys. Rev. Lett. **105**, 133202 (2010).
[28] S. Y. T. van de Meerakker, H. L. Bethlem, and G. Meijer, Nat. Phys. **4**, 595 (2008).
[29] S. D. Hogan, D. Sprecher, M. Andrist, N. Vanhaecke, and F. Merkt, Phys. Rev. A **76**, 023412 (2007).
[30] S. A. Rangwala, T. Junglen, T. Rieger, P. W. H. Pinkse, and G. Rempe, Phys. Rev. A **67**, 043406 (2003).
[31] S. Willitsch, M. T. Bell, A. D. Gingell, S. R. Procter, and T. P. Softley, Phys. Rev. Lett. **100**, 043203 (2008).
[32] M. Drewsen, I. Jensen, J. Lindballe, N. Nissen, R. Martinussen, A. Mortensen, P. Staanum, and D. Voigt, Int. J. Mass Spectrom. **229**, 83 (2003).
[33] R. Alheit, S. Kleineidam, F. Vedel, M. Vedel, and G. Werth, Int. J. Mass Spectrom. Ion Processes **154**, 155 (1996).
[34] S. Seidelin, J. Chiaverini, R. Reichle, J. J. Bollinger, D. Leibfried, J. Britton, J. H. Wesenberg, R. B. Blakestad, R. J. Epstein, D. B. Hume, W. M. Itano, J. D. Jost, C. Langer, R. Ozeri, N. Shiga, and D. J. Wineland, Phys. Rev. Lett. **96**, 253003 (2006).
[35] D. Stick, W. K. Hensinger, S. Olmschenk, M. J. Madsen, K. Schwab, and C. Monroe, Nat. Phys. **2**, 36 (2006).
[36] R. G. DeVoe and C. Kurtsiefer, Phys. Rev. A **65**, 063407 (2002).
[37] S. A. Schulz, U. Poschinger, F. Ziesel, and F. Schmidt-Kaler, New J. Phys. **10**, 045007 (2008).
[38] C. Tamm, D. Engelke, and V. Bühner, Phys. Rev. A **61**, 053405 (2000).
[39] J. J. McLoughlin, A. H. Nizamani, J. D. Siverns, R. C. Sterling, M. D. Hughes, B. Lekitsch, B. Stein, S. Weidt, and W. K. Hensinger, Phys. Rev. A **83**, 013406 (2011).
[40] S. X. Wang, Y. Ge, J. Labaziewicz, E. Dauler, K. Berggren, and I. L. Chuang, Appl. Phys. Lett. **97**, 244102 (2010).
[41] D. M. Lucas, B. C. Keitch, J. P. Home, G. Imreh, M. J. McDonnell, D. N. Stacey, D. J. Szwer, and A. M. Steane, arXiv:0710.4421.